Classification with Scattering Operators

Joan Bruna and Stéphane Mallat
CMAP, Ecole Polytechnique, 91128 Palaiseau

Abstract

A scattering vector is a local descriptor including multiscale and multi-direction co-occurrence information. It is computed with a cascade of wavelet decompositions and complex modulus. This scattering representation is locally translation invariant and linearizes deformations. A supervised classification algorithm is computed with a PCA model selection on scattering vectors. State of the art results are obtained for handwritten digit recognition and texture classification.[1]

1. Introduction

Locally invariant image descriptors such as SIFT [9] provide efficient image representations for image classification and registration [9]. These feature vectors as well as multiscale texture descriptors can be computed with a spatial averaging of wavelet coefficient amplitudes. The averaging reduces the feature variability and provides local translation invariance, but it also reduces information.

Scattering operators recover the lost high frequencies and retransform them into co-occurrence coefficients at multiple scales and orientations. They provide much richer descriptors of complex structures such as corners, junctions and multiscale texture variations. These coefficients are locally translation invariant and they linearize small deformations. They are computed with a convolution network [6] which cascades contractive wavelet transforms and modulus operators [11]. Scattering operators provide new representations of stationary image textures, which can discriminate texture having the same power spectrum.

The scattering transform of a class of signals is approximated by an affine space computed with a PCA. Images are classified by selecting a best approximation space model for their scattering transform. State of the art results are obtained for hand-written digit recognition and for texture discrimination, with important rotation and illumination variability, and small training sets.

Section 2.1 reviews the relations between wavelet transforms and computer vision descriptors. Section 2.2 introduces scattering image representations. Classification by scattering model selection is introduced in Section 3, with numerical results. Softwares are available at `www.cmap.polytechnique.fr/scattering`.

[1]This work is funded by the ANR grant 0126 01.

2. Scattering

A scattering transform computes local image descriptors with a cascade of wavelet decompositions, complex modulus and a local averaging. The resulting scattering representation is locally invariant to translations. It includes coefficients which are similar to SIFT descriptors, together with co-occurrences coefficients at multiple scales and orientations.

2.1. From Wavelets to SIFT and Textons

Image feature vectors such as SIFT and multiscale Gabor textons are obtained by averaging the amplitude of wavelet coefficients, calculated with directional wavelets. Writing these feature vectors as wavelet coefficients helps to understand and to improve their properties.

Let $R_\gamma x$ be the rotation of $x \in \mathbb{R}^2$ by an angle γ. Directional wavelets are obtained by rotating a single ψ, along K angles $\gamma \in \Gamma$. Scaling them by 2^j yields

$$\psi_{j,\gamma}(x) = 2^{-2j}\psi(2^{-j}R_\gamma x) \ .$$

The directional wavelet transform of f at a position x for scales $2^j < 2^J$ is a vector of coefficients

$$W_J f(x) = \begin{pmatrix} f \star \psi_{j,\gamma}(x) \\ f \star \phi_J(x) \end{pmatrix}_{j<J,\gamma\in\Gamma} \qquad (1)$$

where $\phi_J(x) = 2^{-2J}\phi(2^{-J}x)$ is a low-pass filter which carries the low frequencies of f above the scale 2^J: $\int \phi(x)dx = 1$. Let $|W_J f(x)|^2$ be the Euclidean norm of this vector which sums the square of its coordinates. Let $\hat{f}(\omega)$ be the Fourier transform of f. If wavelets satisfy

$$\sum_{j=-\infty}^{-1} \sum_{\gamma\in\Gamma} |\hat{\psi}_\gamma(2^j\omega)|^2 + |\hat{\phi}(\omega)|^2 \leq 1 \qquad (2)$$

then one can verify [11] that

$$\|W_J f\|^2 = \int |W_J f(x)|^2 dx \leq \|f\|^2 = \int |f(x)|^2 \, dx$$

and this inequality is an equality if (2) is an equality. The wavelet transform is then contractive and potentially unitary.

Many standard image feature vectors are obtained by averaging wavelet coefficient amplitudes. SIFT coefficients are obtained from histograms of image gradients calculated at a fine scale 2^j. A histogram bin indexed by $\gamma \in \Gamma$ stores the local sum of the amplitudes of all gradient vectors whose orientations are close to γ. Several authors [15] observed that approximate SIFT feature vectors are computed more efficiently by averaging directly the partial derivative amplitudes of f along the K directions $\gamma \in \Gamma$, with a low-pass filter ϕ_J. These averaged partial derivative amplitudes can be written as averaged wavelet coefficients

$$|f \star \psi_{j,\gamma}| \star \phi_J(x) \, ,$$

with a partial derivative wavelet $\psi(x) = \partial g(x)/\partial x_1$, with $g(x) = e^{-|x|^2/2}$ and $x = (x_1, x_2)$. These averaged wavelet coefficients are nearly invariant to translations or deformations which are small relatively to 2^J.

Partial derivative wavelets are well adapted to detect edge type elements, but these wavelets do not have enough frequency and directional resolution to discriminate more complex structures appearing in textures. For texture analysis, wavelets with a better frequency localization are often used [7]. Complex Gabor functions are examples of such directional wavelets obtained by modulating a Gaussian window at a frequency ξ:

$$\psi(x) = e^{i\xi x_1} \, e^{-|x|^2/2} \, . \tag{3}$$

For stationary textures, $|f \star \psi_{j,\gamma}| \star \phi_J(x)$ has a reduced stochastic variability because of the averaging kernel ϕ_J.

2.2. Scattering Coefficients

The local translation invariance and variability reduction of SIFT descriptors and multiscale textons is obtained by averaging. Scattering operators restore part of the information lost by this averaging with co-occurrence coefficients having similar invariance properties.

The wavelet transform (1) shows that high frequencies eliminated in $|f \star \psi_{j_1,\gamma_1}| \star \phi_J$ by the convolution with ϕ_J are recovered by convolutions with wavelets $|f \star \psi_{j_1,\gamma_1}| \star \psi_{j_2,\gamma_2}$ at scales $2^{j_2} < 2^J$. To become insensitive to local translation and reduce the variability of these coefficients, their complex phase is removed by a modulus, and it is averaged by ϕ_J:

$$||f \star \psi_{j_1,\gamma_1}| \star \psi_{j_2,\gamma_2}| \star \phi_J \, .$$

These are called scattering coefficients because they result from all interferences of f with two wavelets [12]. They give co-occurrence information in f for any pair of scales 2^{j_1}, 2^{j_2} and any two directions γ_1 and γ_2. This can distinguish corners and junctions from edges and it characterizes texture structures. Coefficients are only calculated for $2^{j_2} < 2^{j_1}$ because one can show [11] that $|f \star \psi_{j_1,\gamma_1}| \star \psi_{j_2,\gamma_2}$ is negligible at scales $2^{j_2} \geq 2^{j_1}$.

The convolution with ϕ_J removes high frequencies and thus yields second order coefficients that are locally translation invariant. High frequencies can again be restored by finer scale wavelet coefficients, which are regularized by averaging their amplitude with ϕ_J. Applying iteratively this procedure q times yields a vector of coefficients at each x:

$$S_{q,J} f(x) = \Big(|||f \star \psi_{j_1,\gamma_1}| \star ... \star |\psi_{j_q,\gamma_q}| \star \phi_J(x) \Big)_{\substack{j_1 < ... < j_q < J \\ (\gamma_1,...,\gamma_q) \in \Gamma^q}}$$

This vector has $K^q \binom{J}{q}$ scattering coefficients, computing interactions between f and the successive wavelets $\psi_{j_1,\gamma_1} ... \psi_{j_q,\gamma_q}$. A scattering vector aggregates all these coefficients up to a maximum order $q \leq m$:

$$S_J f(x) = \Big(S_{q,J} f(x) \Big)_{0 \leq q \leq m} \, ,$$

and the first coefficient is the signal average $S_{0,J} f(x) = f \star \phi_J(x)$. The scattering vector size is $\sum_{q=0}^{m} K^q \binom{J}{q}$. After convolution with ϕ_J the output is subsampled at intervals 2^J. If $f(n)$ is an image of N pixels, this uniform sampling yields a scattering representation $S_J f(2^J n)$ including a total of $N_J = 2^{-2J} N \sum_{q=0}^{m} K^q \binom{J}{q}$ coefficients.

A scattering vector is computed with a cascade of convolutions and modulus operators over $m+1$ layers, like in convolution network architectures [6, 1]:

$$\begin{array}{ccc} f(n) & \rightarrow & f \star \phi_J(2^J n) \\ \downarrow & & \\ |f \star \psi_{j_1,\gamma_1}| & \rightarrow & |f \star \psi_{j_1,\gamma_1}| \star \phi_J(2^J n) \\ \downarrow & & \\ ||f \star \psi_{j_1,\gamma_1}| \star \psi_{j_2,\gamma_2}| & \rightarrow & ||f \star \psi_{j_1,\gamma_1}| \star \psi_{j_2,\gamma_2}| \star \phi_J(2^J n) \\ \downarrow & & \\ ... & & \end{array}$$

To reduce computations, wavelet convolutions are subsampled at intervals proportional to the last scale 2^{j_q}, with an oversampling factor of 2:

$$|||f \star \psi_{j_1,\gamma_1}| \star ... \star |\psi_{j_q,\gamma_q}(2^{j_q - 1} n)| \, .$$

A final low-pass filtering and subsampling yields

$$|||f \star \psi_{j_1,\gamma_1}| \star ... \star |\psi_{j_q,\gamma_q}| \star \phi_J(2^J n)$$

With an FFT, the overall computational complexity is then $O(N \log N)$.

2.3. Scattering Distance and Deformation Stability

The scattering transform defines a distance between two images f and g. This distance has important invariance and stability properties that are briefly reviewed. Let $|S_J f(x)|^2$ be the squared Euclidean norm of the vector $S_J f(x)$. The scattering distance of f and g is

$$\|S_J f - S_J g\|^2 = \int |S_J f(x) - S_J g(x)|^2 \, dx. \quad (4)$$

For discrete images, the integral is replaced by a discrete sum. The scattering operator S_J is contractive because it is a cascade of wavelet transforms W_J and modulus operators, which are both contractive [8]:

$$\|S_J f - S_J g\|^2 \leq \|f - g\|^2 = \int |f(x) - g(x)|^2 \, dx \; .$$

In particular $\|S_J f\|^2 \leq \|f\|^2$. If the maximum order is $m = \infty$ then one can prove [11] that if the wavelet transform is unitary then for appropriate complex wavelets $\|S_J f\|^2 = \|f\|^2$. The energy of f is thus spread across scattering coefficients of multiple orders, but this energy has a fast decay as the co-occurrence order q increases. In the Caltech101 image database, 98% of the energy $\|S_J f\|^2$ is carried by scattering coefficients of order 0, 1 and 2. In applications, we shall thus limit the scattering order to $m = 2$. The energy of all scattering coefficients of order 2, $||f \star \psi_{j_1,\gamma_1}| \star \psi_{j_2,\gamma_2}| \star \phi_J$, is about 20% of the energy of all order 1 coefficients $|f \star \psi_{j_1,\gamma_1}| \star \phi_J$, which is not negligible. We shall see that order 2 coefficients have indeed an important impact on classification results.

The efficiency of a scattering representation comes from its invariance to local translations due to convolutions with ϕ_J, and from its ability to linearize deformations. Let $D_\tau f(x) = f(x - \tau(x))$ be a deformation of f with a regular displacement field $\tau(x)$. It is a pure translation only if $\nabla\tau = 0$. We write $|\tau|_\infty = \sup_x |\tau(x)|$ the maximum translation amplitude, and $|\nabla\tau|_\infty = \sup_x |\nabla\tau(x)|$ the maximum deformation amplitude, where $|\nabla\tau(x)|$ is the matrix sup norm of $\nabla\tau(x)$. The sup-norm of the Hessian of τ is also written $|H\tau|_\infty$. It is shown in [11] that the scattering metric satisfies

$$\|S_J(D_\tau f) - S_J f\| \leq Cm\|f\|\Big(2^{-J}|\tau|_\infty + J(|\nabla\tau|_\infty + |H\tau|_\infty)\Big). \quad (5)$$

The first term $2^{-J}|\tau|_\infty$ is the translation error which is small if $2^J \gg |\tau|_\infty$. The other terms are dominated by the deformation amplitude $|\nabla\tau|_\infty$. If $2^J \geq |\tau|_\infty / |\nabla\tau|_\infty$ then two deformed signals have a scattering distance essentially proportional to the deformation amplitude $|\nabla\tau|_\infty$.

3. Classification by Affine Model Selection

A scattering representation $S_J f$ is invariant to small translations relatively to 2^J. It linearizes deformations and provides co-occurence descriptors. A classifier is obtained by selecting an affine space model which best approximates $S_J f$.

Each signal class is represented by a random vector F_i whose realizations are images of N pixels in the class. Scattering vectors $S_J F_i(2^J n)$ define an image representation with a total of $N_J = 2^{-2J} N \sum_{q=0}^{m} K^q \binom{J}{q}$ coefficients. Let $E\{S_J F_i(2^J n)\}$ be their expected values. Deformations of F_i are mostly linearized by S_J and thus produce a variability $S_J F_i - E\{S_J F_i\}$ which is well approximated in a linear space of low dimension d. This linear space is computed with a PCA by diagonalizing the covariance of $S_J F_i$. We denote by $\mathbf{V}_{d,i}$ the space generated by the d covariance eigenvectors of largest variance. The dimension d is adjusted so that $S_J F_i$ is closely approximated by its projection in the affine space

$$\mathbf{A}_{d,i} = E\{S_J F_i\} + \mathbf{V}_{d,i} \; .$$

in comparison with the error produced by the affine spaces $\mathbf{A}_{d,i'}$, $i' \neq i$, corresponding to the other classes.

A signal f will be associated to the class $\hat{\imath}$ which yields the best affine space approximation:

$$\hat{\imath}(f) = \operatorname*{argmin}_{i \leq I} \|S_J f - P_{\mathbf{A}_{d,i}}(S_J f)\| \; . \quad (6)$$

Observe that

$$\|S_J f - P_{\mathbf{A}_{d,i}}(S_J f)\| = \|P_{\mathbf{V}_{d,i}^\perp}(S_J f - E\{S_J F_i\})\|$$

where $\mathbf{V}_{d,i}^\perp$ is the orthogonal complement of $\mathbf{V}_{d,i}$. Minimizing the affine space approximation error is thus equivalent to minimize the distance between $S_J f$ and the class centroid $E\{S_J F_i\}$, without taking into account the first d principal variability directions. A cross-validation procedure finds the dimension d and the scale 2^J which yields the smallest classification error. This error is computed on a subset of the training images that is not used for the PCA calculations.

Affine space scattering models can be interpreted as generative models computed independently for each class. As opposed to discriminative classifiers such as an SVM, no interaction between classes is taken into account, besides the choice of the model dimensionality d.

Classification results are given for hand-written digits and textures that are deformed, rotated, scaled and have illumination variations. Scattering descriptors are computed with the complex Gabor wavelet (3) for $\xi = 3\pi/4$, rotated along angles $k\pi/K$ with $0 \leq k < K = 6$. The lowpass filter is the Gaussian $\phi_J(x) = \lambda_J \exp(-(3x/2^{J+1})^2/2)$ with $\int \phi_J(x)dx = 1$.

3.1. Handwritten digit recognition

The MNIST database of hand-written digits is an example of structured pattern classification, where most of the

Table 1. Percentage of error as a function of the training size for MNIST, for a Convolution Network [14], an SVM over scattering coefficient for $m = 2$, a PCA for $m = 1, 2, 3$. Minimum errors are in bold.

Training size	Conv. Net.	SVM $m = 2$	PCA $m = 1$	PCA $m = 2$	PCA $m = 3$
300	7.18	21.5	7.03	6.05	**5.97**
1000	3.21	3.06	2.99	2.39	**2.37**
2000	2.53	1.87	2.11	1.71	**1.71**
5000	1.52	1.54	1.85	1.57	**1.22**
10000	**0.85**	1.15	1.61	1.17	0.99
20000	**0.76**	0.92	1.4	0.96	0.82
40000	**0.65**	0.85	1.32	0.78	0.79
60000	**0.53**	0.7	1.4	0.77	0.72

Table 2. Values of the dimension d of affine approximation models, of the intra class normalized approximation error σ_d^2, and of the ratio λ_d between inter class and intra class approximation errors, as a function of the training size.

Training	d	σ_d^2	λ_d
300	24	$2 \cdot 10^{-2}$	2.4
5000	40	$5 \cdot 10^{-3}$	3.6
40000	180	$6 \cdot 10^{-4}$	4.3

intra-class variability is due to local translations and deformations. It comprises at most 60000 training samples and 10000 test samples. The state of the art is achieved with deep-learning convolutional networks [14] and dictionary learning [10].

Table 1 compares the scattering PCA classifier at maximum orders $m = 1$, $m = 2$ and $m = 3$. Cross validation finds an optimal scattering scale $2^J = 2^3$. This value is compatible with observed deformations of digits whose amplitude is typically at most 8 pixels. For $J = 3$, there are $N/64$ second order scattering vectors $S_J f$ of dimension 127 each.

Below $5\,10^3$ training samples, the scattering PCA classifier improves results of deep-learning convolutional networks. For $m = 2$, second order scattering coefficients improve classification results obtained with $m = 1$, but a third order $m = 3$ scattering yields marginal improvements. An SVM classifier is also applied on scattering vectors for $m = 2$, with a polynomial kernel whose degree was optimized. Minimum errors are obtained with a degree 4. The SVM error is well above the PCA model selection error up to 60000 samples. For small training sets, it was indeed shown [13] that generative models, which do not estimate cross terms between classes, can outperform discriminative classifiers such as SVM.

Table 3. Percentage of errors on an MNIST rotated dataset [5].

PCA $m = 1$	PCA $m = 2$	PCA $m = 3$	Conv. Net.
6.3	3	**2.8**	8.8

Table 4. Percentage of errors for the whole USPS database.

Tang. Kern.	SVM $m = 2$	PCA $m = 1$	PCA $m = 2$	PCA $m = 3$
2.4	2.64	3.24	2.74	2.74

Table 2 gives the dimension d of affine approximation spaces calculated by cross validation, for $m = 2$. The normalized approximation error σ_d^2 is the expected approximation error $E\{\|S_J F_i - P_{\mathbf{A_{i,d}}}(S_J F_i)\|^2\}$ in a class i divided by the squared norm of $S_J F_i$, averaged over all i and all F_i in the test set. Table 2 shows that the cross-validation calculation of d yields small approximation errors. Table 2 also gives the relative approximation error

$$\lambda_d = \frac{E\{\min_{i' \neq i} \|S_J F_i - P_{\mathbf{A_{i',d}}}(S_J F_i)\|^2\}}{E\{\|S_J F_i - P_{\mathbf{A_{i,d}}}(S_J F_i)\|^2\}}$$

produced by the closest affine model of a different class than that of F_i, averaged over all classes. As expected, when the training set increases, the dimension d increases so σ_d^2 decreases and the relative approximation error λ_d increases, which reduces the error rate.

Rotation invariance in the MNIST database is studied in the same setting as in [5]. The authors have constructed a transformed database with 12000 training samples and 50000 test images, where samples are rotated versions of the digits using a uniform distribution in $[0, 2\pi]$. The PCA incorporates rotation invariance by increasing the dimension d of the affine space $\mathbf{A}_{i,d}$. It removes the main variability directions of $S_J f$ due to rotations. Error rates in Table 3 are smaller with a scattering PCA than with a convolution network [5]. Better results are obtained with $m = 2$ than with $m = 1$ because second order coefficients maintain enough discriminability despite the removal of a larger number d of principal directions.

The US-Postal Service dataset is another handwritten digit dataset, with 7291 training samples and 2007 test images 16×16 pixels. The state of the art is obtained with tangent distance kernels [2]. Table 4 gives results obtained with the PCA classifier and a polynomial kernel SVM classifier applied to scattering coefficients. The scattering scale was also set to $J = 3$ by cross-validation.

3.2. Scattering Texture Classification

Scattering coefficients provide new texture descriptors, carrying co-occurrence information at different scales and

orientations. A texture can be modeled as a realization of a stationary process $F(x)$. Scattering coefficients $S_J F(x)$ are obtained with successive convolutions and modulus operators which preserve stationarity. Averaging by ϕ_J does not modify expected values so $E\{S_J F(x)\}$ is a vector whose coefficients do not depend upon x and ϕ_J. The convolution with ϕ_J reduces the coefficient variability and for a large class of ergodic processes, the variance of $S_J F(x)$ decreases exponentially to zero as J increases. As a result, $S_J F(x)$ is a good estimator of $E\{S_J F(x)\}$ when J is sufficiently large. Figure 1 shows an example of such vector for a textured image with $m = 3$.

Figure 1. The right plot gives scattering coefficients, ordered according to their scattering order q. Blue coefficients correspond to $q = 1$, green coefficients correspond to $q = 2$ and red coefficients to $q = 3$. Notice the exponential amplitude decay as the order increases.

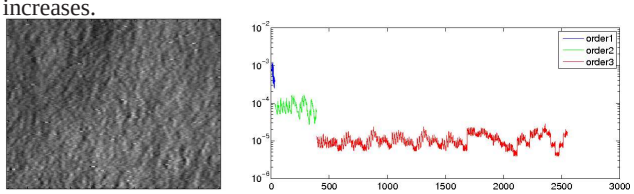

Textures having same mean and same power spectrum have nearly the same scattering coefficients of order $q = 0$ and $q = 1$. However, different textures typically have cooccurence coefficients of order $q \geq 2$ which are different. Let $S_{q,J} F_i$ be the vector of scattering coefficients of order q for a texture F_i. The distance of scattering vectors of order q for two textures F_1 and F_2 is normalized by their variance $\sigma^2(S_{q,J} F_i)$:

$$\rho_q(F_1, F_2) = \frac{|E\{S_{q,J} F_1\} - E\{S_{q,J} F_2\}|^2}{\sigma^2(S_{q,J} F_1) + \sigma^2(S_{q,J} F_2)} \, .$$

Table 5 gives $\rho_q(F_1, F_2)$ for two Brodatz textures in Figure 2, which have different power spectrum. Their expected scattering vectors $E\{S_J F_{q,i}\}$ have a relatively large distance $\rho_q(F_1, F_2)$ at all orders $q \geq 1$. The texture $\widetilde{F}_1$ in Figure 2 has same power spectrum as F_2. When $q = 1$, equalizing the power spectrum reduces $\rho_q(\widetilde{F}_1, F_2)$ to 0 (up to estimation errors) but $\rho_q(\widetilde{F}_1, F_2)$ remains well above zero for $q > 1$. Textures having same power spectrum can thus be discriminated from scattering coefficients of order $q > 1$.

Texture classification is tested on the CUReT texture database [7, 16], which includes 61 classes of image textures of $N = 200^2$ pixels. Each texture class gives images of the same material with different pose and illumination conditions. Specularities, shadowing and surface normal variations make it challenging for classification. Pose variations require global rotation invariance. Figure 3 illustrates the large intra class variability, and also shows that the variability across classes is not always important.

Figure 2. Left and right Brodatz textures $F_1$and F_2 have different power spectrum. The middle texture $\widetilde{F}_1$ is obtained by filtering F_1 to equalize its power spectrum with F_2.

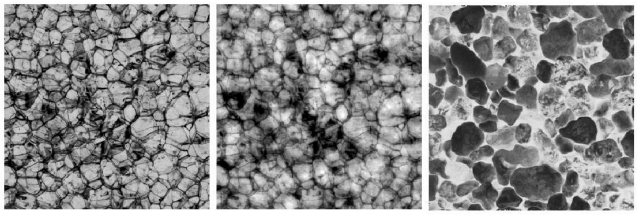

Table 5. Normalized distance ρ_q of expected scattering vectors of order q, for textures in Figure 2.

q	$\rho_q(F_1, F_2)$	$\rho_q(\widetilde{F}_1, F_2)$
1	12	0
2	12	1
3	6	2
4	3	2

State of the art on this database achieves a 2.46% error rate, obtained in [16] with an optimized Markov Random Field model. The scattering PCA classifier has a 0.09% error rate, which is a factor 25 improvement, as shown in Table 6. The database is randomly split into a training and a testing set, which either comprises 46 training images each as in [16], or contains 23 training images as in [3]. Results are averaged over 10 different splits.

The cross-validation adjusts the scattering scale $2^J = 2^7$ which is the maximum value. Indeed, these textures are fully stationary and increasing the scale reduces the vari-

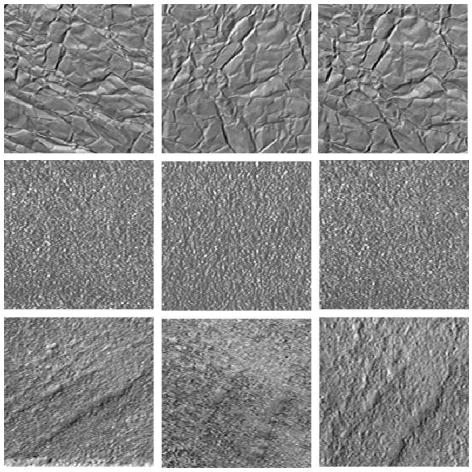

Figure 3. Examples of textures from the CUReT database. Each row shows a different class, showing intra-class variability in the form of stochastic variability and changes in pose and illumination.

Table 6. Percentage of errors on CUReT for different training sizes.

Training size	PCA $m = 2$	SVM $m = 2$	LBP [3]	Mark. Rand. 8
23	$\mathbf{0.9 \pm 0.1}$	3.3	18.23	22.43
46	$\mathbf{0.09 \pm 0.05}$	1.7	3.96	2.46

ance of the scattering coefficients variability across realizations. Global invariance to rotation and illumination is provided by the PCA affine space models. They include the main variation directions of scattering vectors due to rotations or illumination variations.

The dimension of affine approximation space models is adjusted by cross validation to $d = 6$ and $d = 22$ respectively for 23 and 46 training samples. The resulting error rates are respectively 0.9% and 0.09%. With an SVM, the classification error for 46 training samples per class increases to 1.7%. For 46 training samples, the intra class normalized approximation error σ_d^2 is only $2.5 \cdot 10^{-3}$, about half of the error produced in the case of 23 training samples, in which σ_d^2 is $5.3 \cdot 10^{-3}$. Such low approximation error has been possible thanks to the fast variance decay of scattering coefficients as the scale increases and to the global invariance properties of the affine spaces.

4. Conclusion

A scattering transform provides a locally translation invariant representation, which linearizes small deformations, and provides co-occurrence coefficients which characterize textures. For handwritten digit recognition and texture discrimination with small training size sequences, a PCA model selection classifier yields state of the art results.

Besides translations, invariance can be extended to any compact Lie group G, by combining another scattering transform defined on G. The cascade of wavelet transforms in $\mathbf{L^2}(\mathbf{R^2})$ is then replaced by a cascade of wavelet transforms in $\mathbf{L^2}(G)$ [11].

References

[1] J. Bouvrie, L. Rosasco, T. Poggio: "On Invariance in Hierarchical Models", NIPS 2009.

[2] B.Haasdonk, D.Keysers: "Tangent Distance kernels for support vector machines", 2002.

[3] Guo,Z., Zhang, L., Zhang,D., "Rotation Invariant texture classification using LBP variance (LBPV) with global matching", Elsevier Journal of Pattern Recognition, Aug. 2009.

[4] K. Jarrett, K. Kavukcuoglu, M. Ranzato and Y. LeCun: "What is the Best Multi-Stage Architecture for Object Recognition?", Proc. of ICCV 2009.

[5] Larochelle, H., Bengio, Y., Louradour, J., Lamblin, P., "Exploring Strategies for Training Deep Neural Networks", Journal of Machine Learning Research, Jan. 2009.

[6] Y. LeCun, K. Kavukvuoglu and C. Farabet: "Convolutional Networks and Applications in Vision", Proc. of ISCAS 2010.

[7] T. Leung, and J. Malik; "Representing and Recognizing the Visual Appearance of Materials Using Three-Dimensional Textons". International Journal of Computer Vision, 43(1), 29-44; 2001.

[8] W. Lohmiller and J.J.E. Slotine "On Contraction Analysis for Nonlinear Systems", Automatica, 34(6), 1998.

[9] Lowe, D. G., "Distinctive Image Features from Scale-Invariant Keypoints", International Journal of Computer Vision, 60, 2, pp. 91-110, 2004

[10] Mairal, J., Bach, F., Ponce, J. , "Task-Driven Dictionary Learning", Submitted to IEEE trans. on PAMI, September 2010.

[11] S. Mallat "Group Invariant Scattering", http://arxiv.org/abs/1101.2286.

[12] S. Mallat, "Recursive Interferometric Representation", Proc. of EUSICO conference, Denmark, August 2010.

[13] A. Y. Ng and M. I. Jordan "On discriminative vs. generative classifiers: A comparison of logistic regression and naive Bayes", in Advances in Neural Information Processing Systems (NIPS) 14, 2002.

[14] M. Ranzato, F.Huang, Y.Boreau, Y. LeCun: "Unsupervised Learning of Invariant Feature Hierarchies with Applications to Object Recognition", CVPR 2007.

[15] Tola, E., Lepetit, V., Fua, P., "DAISY: An Efficient Dense Descriptor Applied to Wide-Baseline Stereo", IEEE trans on PAMI, May 2010.

[16] M.Varma, A. Zisserman: "A Statistical Approach To Material Classification Using Image Patch Exemplars". IEEE Trans. on PAMI, 31(11):2032–2047, November 2009.